ISIJ International, Vol. 45 (2005), No. 12, pp. 1903–1908

An Analysis of the Transition between Strain Dependent and Independent Softening in Austenite

Mark R. CARTMILL, Matthew R. BARNETT, Saden H. ZAHIRI[1)] and Peter D. HODGSON

School of Engineering and Technology, Deakin University, Geelong, Victoria 3217, Australia. E-mail: mrcar@deakin.edu.au, barnettm@deakin.edu.au, phodgson@deakin.edu.au 1) CSIRO Manufacturing and Infrastructure Technology, Private Bag 33, Clayton South, Victoria 3169, Australia. E-mail: Saden.Zahiri@csiro.au

(*Received on June 27, 2005; accepted on August 11, 2005*)

The post-deformation softening behaviour of austenite has been studied for various compositions and deformation conditions. The strain at which the transition from strain dependent to strain independent post-deformation softening behaviour occurs (ε^*) has been found to coincide closely with the strain to the peak stress (ε_p) under certain conditions but not under others. It has been proposed that the relationship between ε^* and ε_p may be described geometrically using the initial grain size and the dynamically recrystallised grain size.

KEY WORDS: static recrystallisation; metadynamic recrystallisation; dynamic recrystallisation; peak strain.

1. Introduction

It has been widely accepted that the post-deformation softening kinetics of austenite may be separated into two modes (ignoring recovery which plays only a minor role in austenite)—static recrystallisation and metadynamic recrystallisation. Static recrystallisation involves both nucleation and growth of newly recrystallised grains,[1)] whereas metadynamic recrystallisation has been defined as the continued growth of nuclei formed during dynamic recrystallisation (DRX).[2)]

It is also well known that the softening following deformation is strain dependent at low strains but strain independent at high strains, with a transition between the two behaviours occurring at a characteristic strain, ε^*.[3)] This critical strain has been variously assumed to coincide with either the strain corresponding to the flow stress peak ("peak strain"), ε_p,[4)] or the critical strain for the initiation of DRX, ε_c.[5–7)] Others have reported that the transition strain follows the peak strain according to $\varepsilon^*=K\varepsilon_p$, where the value of K is 1.5,[3,8,9)] 1.7[10)] or dependent upon Z.[11)]

The objective of this paper is to examine more closely the correlation between ε^* and the critical strains obtained from the stress–strain curves for a range of steels. The aim is twofold: i) to provide equations of use to industry and ii) to gain insight into what determines ε^*.

2. Experimental

Three commercial grades of steel were chosen for this investigation: a C–Mn grade, a HSLA grade and an IF grade. The compositions are shown in **Table 1**. Torsion samples 20 mm in length and 6.7 mm in diameter were machined from transfer bar crop ends obtained from BlueScope Steel's Westernport hot strip mill and were mechanically tested using a computer controlled hot torsion machine. The torsion apparatus and general test procedure has been described elsewhere.[12)]

The deformation schedule carried out on the torsion machine consisted of reheating the specimen to 1 200°C for the C–Mn grade and 1 250°C for the HSLA and IF grade (thereby, according to solute equations, ensuring complete dissolution of niobium precipitate particles) and holding at this temperature for 5 min. The specimen was then cooled at 2°C s^{-1} until a temperature of 1 100°C was attained, whereupon two roughing passes were carried out, each to a strain of 0.4 at a strain rate of 1 s^{-1} separated by an inter-deformation delay of 40 s. This ensured a consistent grain size for each of the three grades.

Once the roughing deformation had been applied, the sample was cooled at 2°C s^{-1} until the desired deformation temperature was reached. The softening kinetics were then obtained for a range of strains and strain rates using conventional 'double hit' methods.[13)]

Microstructural analysis was also performed for a range of selected conditions; a process that involved quenching the samples using high pressure water sprays and etching the subsequently cut and polished cross-sections using a heated (≈100°C) solution of picric acid, water and Teepol to reveal the prior austenite structure.[14)] The average linear

Table 1. Composition (wt%) of steels used in this study.

Grade	C	Mn	P	Al	S	Ti	Nb	N
C-Mn	0.055	0.209	0.011	0.037	0.013	0.003	0.001	0.003
HSLA	0.083	0.765	0.010	0.034	0.005	0.022	0.024	0.022
IF	0.002	0.144	0.009	0.040	0.011	0.083	0.001	0.003

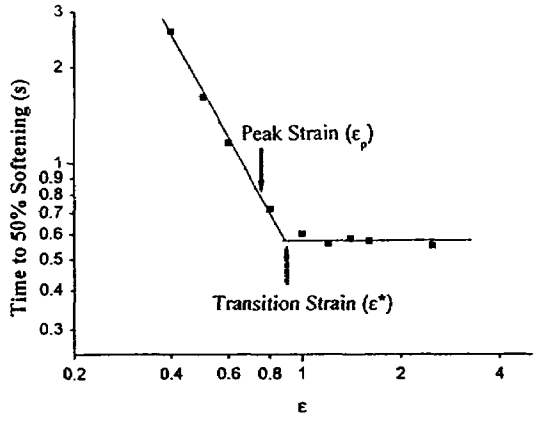

Fig. 1. Time to 50% softening as a function of strain for the IF grade deformed at $\dot{\varepsilon}=1\ s^{-1}$ and 975°C.

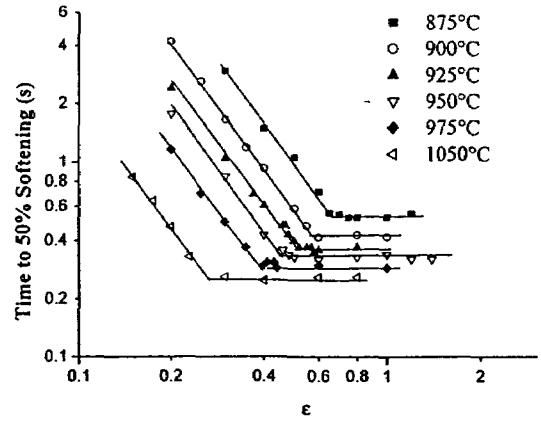

Fig. 2. Effect of temperature on time to 50% softening for the C–Mn grade deformed at $\dot{\varepsilon}=1/s$ with an initial grain size≈70 μm.

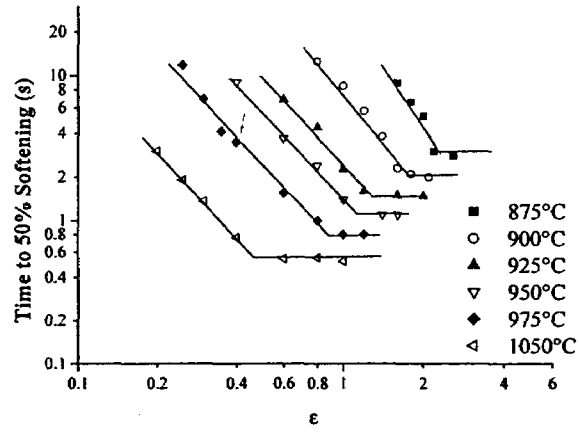

Fig. 3. Effect of temperature on time to 50% softening for the HSLA grade deformed at $\dot{\varepsilon}=1/s$ with an initial grain size≈45 μm.

intercept grain size was then determined based on 10 random fields located 100 μm or less from the surface of each sample. The grain sizes determined for the C–Mn, HSLA and IF grades after roughing were 70 μm, 45 μm and 55 μm respectively, with very little variation over the temperature range used.

3. Results

Interrupted torsion tests were used to examine the effect of strain, strain rate, temperature and initial grain size upon the softening kinetics of the three grades. The relative softening, X (%), was determined from the expression:

$$X(\%)=\frac{(\sigma_m-\sigma_2)}{(\sigma_m-\sigma_1)}\times 100 \quad \text{.....(1)}$$

where σ_m is the stress at the end of first deformation, σ_1 is 0.2% offset yield stress for the first deformation and σ_2 is 0.2% offset yield stress for the second deformation. A rapid method of determining softening kinetics through the analysis of the time to 50% softening ($t_{0.5}$) was adopted for this analysis (the details of which are described elsewhere[11]). The general features of the data generated by this method may be seen in **Fig. 1**. The most obvious feature in this figure is the sharp change in softening behaviour once an applied strain of 0.85 is exceeded, with further deformation exerting no significant influence over the softening kinetics. The strain to the flow stress peak for these conditions falls at a strain of 0.7. In this case the transition strain (ε^*) was higher than the peak strain by a factor of 1.2.

The softening in the strain dependent region was modelled using a power law equation with the general form.[1]

$$t_{0.5}=B\varepsilon^{-p}\dot{\varepsilon}^{-q}d_0^r\exp\left(\frac{Q_{rex}}{RT}\right) \quad \text{.....(2)}$$

where ε=applied strain
$\dot{\varepsilon}$=strain rate (s^{-1})
d_0=initial austenite grain size
Q_{rex}=apparent recrystallisation activation energy (J/mol)
R=gas constant (8.31 J·mol/K)
T=deformation temperature (K)
B, p, q, r=material dependent constants

The softening kinetics in the strain independent region were modelled using an equation of the form:

$$t_{0.5}=C\dot{\varepsilon}^{-q}\exp\left(\frac{Q_{rex}}{RT}\right) \quad \text{.....(3)}$$

The determination of the various exponents and coefficients of the two regions is discussed below.

3.1. Effect of Strain and Temperature

The effect of temperature upon the softening kinetics of each of the three grades can be seen in **Figs. 2, 3 and 4**. In all cases the strain exponent for the strain dependent region was 2. As expected, increasing the temperature accelerated the kinetics of softening in all three grades. The apparent recrystallisation activation energies are given in **Table 2** and it can be seen that strain independent softening is significantly less affected by temperature then strain dependent softening.

3.2. Effect of Strain Rate

The effect of strain rate upon the time to 50% softening for each of the three grades is shown in **Figs. 5, 6 and 7**. It may be observed in all three grades that strain rate exerts a significant influence over the post-ε^* softening kinetics and a lesser (though not negligible) influence over the pre-ε^* softening kinetics. The relevant power law exponents are provided in Table 2.

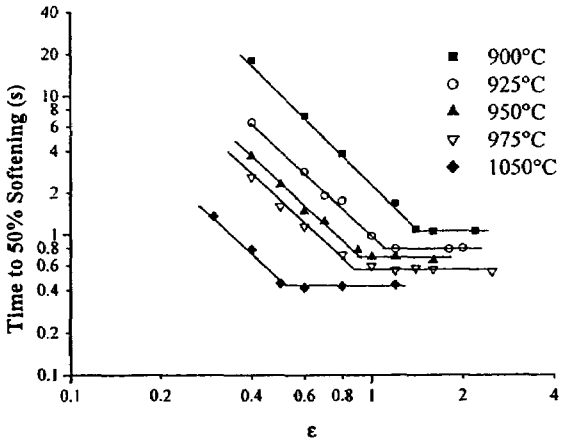

Fig. 4. Effect of temperature on time to 50% softening for the IF grade deformed at $\dot{\varepsilon}$=1/s with initial grain size≈55 μm.

Table 2. Softening equations for tested grades.

Grade	Strain Dependent Softening	Strain Independent Softening
C-Mn	$t_{50}=9.57\times10^{-3}\varepsilon^{-2}\dot{\varepsilon}^{-0.34}d_o^{2}\exp\left(\frac{215000}{RT}\right)$	$t_{50}=9.11\times10^{-5}\dot{\varepsilon}^{-0.8}\exp\left(\frac{83000}{RT}\right)$
HSLA	$t_{50}=4.48\times10^{-4}\varepsilon^{-2}\dot{\varepsilon}^{-0.37}d_o^{2}\exp\left(\frac{330000}{RT}\right)$	$t_{50}=9.4\times10^{-5}\dot{\varepsilon}^{-0.83}\exp\left(\frac{97000}{RT}\right)$
IF	$t_{50}=1.05\times10^{-11}\varepsilon^{-2}\dot{\varepsilon}^{-0.37}d_o^{2}\exp\left(\frac{250000}{RT}\right)$	$t_{50}=7.62\times10^{-4}\dot{\varepsilon}^{-0.8}\exp\left(\frac{70000}{RT}\right)$

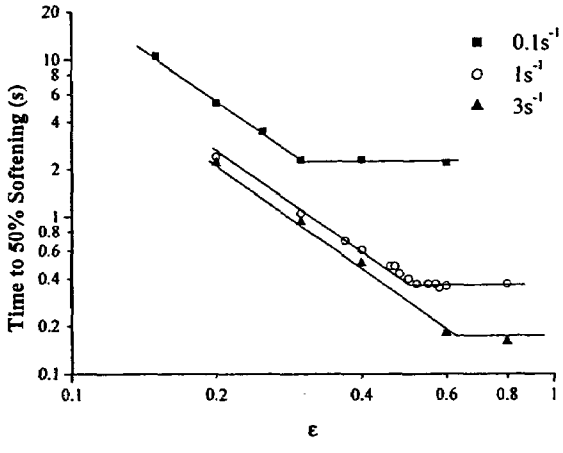

Fig. 5. Effect of strain rate (SR) on time to 50% softening for the C–Mn grade at T=925°C with an initial grain size≈70 μm.

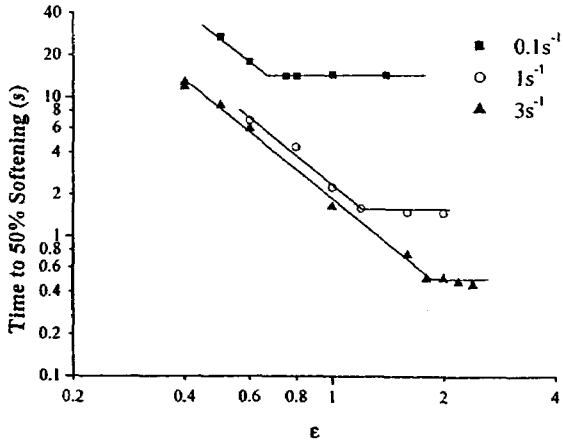

Fig. 6. Effect of strain rate (SR) on time to 50% softening for the HSLA grade at T=925°C with an initial grain size≈45 μm.

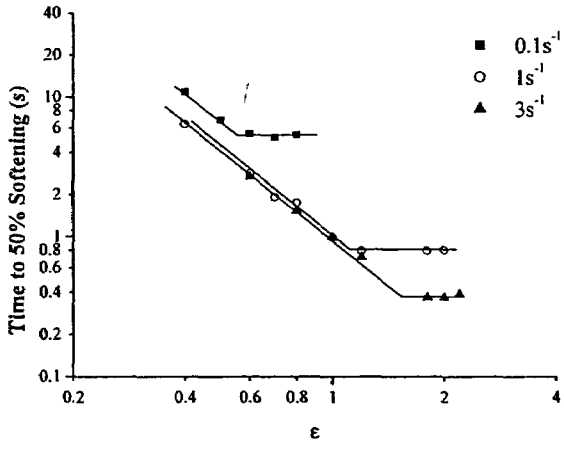

Fig. 7. Effect of strain rate (SR) on time to 50% softening for the IF grade at T=925°C with an initial grain size≈55 μm.

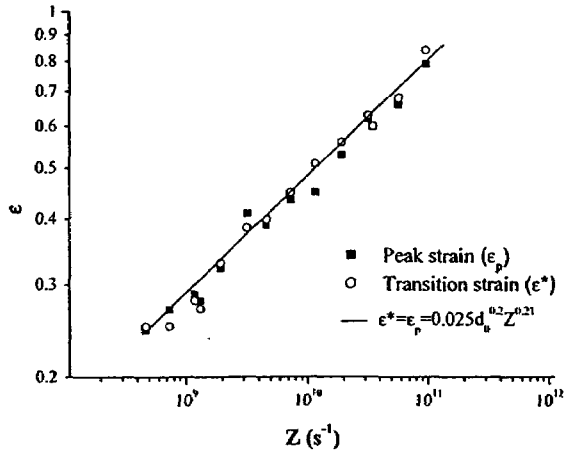

Fig. 8. Strains corresponding to the flow stress peak (ε_p) and the softening transition (ε^*) plotted against Z for the C–Mn grade (Q_{def}=231 kJ/mol).

3.3. Effect of Zener–Hollomon Parameter (Z) on the Relationship between Transition Strain (ε^*) and Peak Strain (ε_p)

Values of ε_p and ε^* are plotted in **Figs. 8–10**. In the C–Mn grade (Fig. 8), the two strains coincide but for the HSLA and IF grades, ε^* exceeds ε_p at higher values of Z. In these grades, the ratio $\varepsilon_p/\varepsilon^*$ increases with Z. The data can be described using the general form of the equation developed by Sellars[15] that relates peak strain to the initial grain size (d_0) and the Zener–Hollomon parameter:

$$\varepsilon_p=Bd_0^mZ^r \quad \text{.....(4)}$$

where B is a material dependent constant, the grain size exponent m was calculated to be approximately 0.2 for the IF grade (which falls within the range cited in the literature of 0.147[16] to 0.5[15]) and the Z exponent r was calculated to be approximately 0.21 for all three grades (which falls within the range cited in the literature of 0.12 to 0.22.[17]). As may be seen in Figs. 8–10, ε^* was also observed to display a

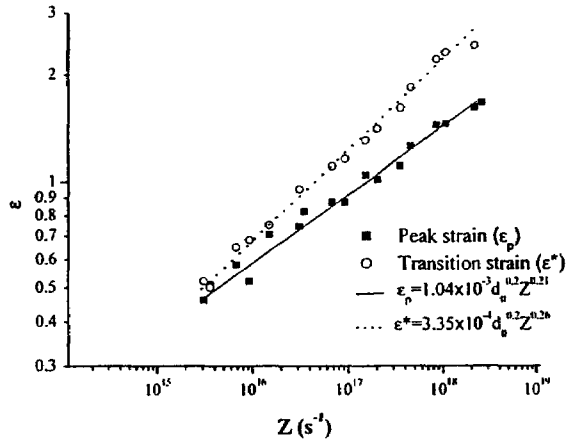

Fig. 9. Strains corresponding to the flow stress peak (ε_p) and the softening transition (ε^*) plotted against Z for the HSLA grade (Q_{def}=394 kJ/mol).

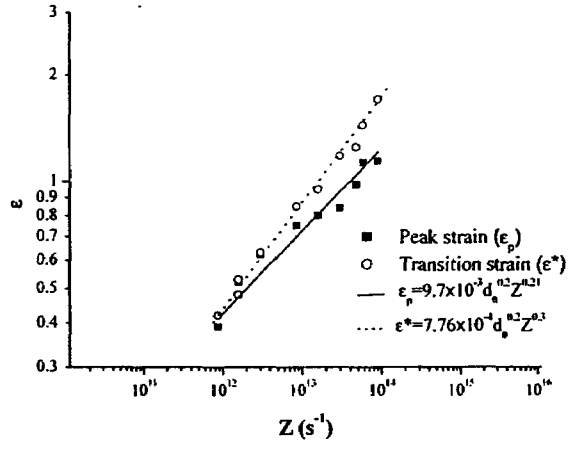

Fig. 10. Strains corresponding to the flow stress peak (ε_p) and the softening transition (ε^*) plotted against Z for the IF grade (Q_{def}=309 kJ/mol).

power law dependency upon Z (and presumably d_0), although for reasons discussed later this relationship would be expected to be made up of two regions of different slopes.

4. Discussion

4.1. Kinetics of Strain Dependent Softening

The observed characteristics of strain dependent softening kinetics for the three grades examined in this study are in good agreement with the literature[3,8,10,11]; namely that strain, grain size and temperature each exert a strong influence upon softening times, while strain rate exerts a weak (although not negligible) influence.

As may be noted from comparing the experimentally determined softening activation energies of the three grades given in Table 2, the strain dependent softening kinetics of the HSLA grade (Q_{rex}=330 kJ/mol) display a far greater dependence upon temperature than either the IF grade (Q_{rex}= 250 kJ/mol) or the C–Mn grade (Q_{rex}=215 kJ/mol). This may be attributed to the niobium content of the HSLA grade, with the drag effect of the niobium solute atoms expected to increase as the temperature is reduced.[18]

It is also of interest that, although the IF grade has quite a high titanium content compared to the other two grades, it displays a temperature sensitivity of softening not considerably higher than the C–Mn grade. This has been observed previously in the literature,[19–21] with Medina *et al.*[20] attributing this low solute drag effect to the solution temperature of large titanium nitrides being greater than 1 250°C[22] and therefore not dissolving at the reheating temperature used in this study.

The effect of strain rate upon strain dependent softening is also consistent with the literature,[23] with the experimentally determined strain rate exponent q for the C–Mn and IF grade (q=0.34) and the HSLA grade (q=0.37) comparing well with the values reported by Zahiri *et al.*[18] (q=0.4) and Sun *et al.*[24] (q=0.33).

4.2. Kinetics of Strain Independent Softening

The kinetics of strain independent softening observed here largely depended upon strain rate and, to a lesser degree, temperature. This was expected.[2,13,18,24] The strain rate exponents of 0.8 for the C–Mn and IF grade and 0.83 for the HSLA grade are quite similar to values reported by Hodgson *et al.*[25] (0.8 for both C–Mn and Nb grades), Zahiri *et al.*[18] (0.8 for an IF grade) and Cho *et al.*[26] (0.84 for a Nb grade).

It is also apparent from the relative softening activation energies of the three grades that composition is not a major consideration in determining the influence of temperature on strain independent softening. Furthermore, the 'apparent' activation energies for strain dependent softening are lower than those obtained in the strain dependent region. This arises from the fact that this term reflects the competing effects of temperature on the initial structure and the recrystallization reaction itself. The deformed structure in the strain independent region is more sensitive to temperature than the strain dependent region due to temperature affecting the high angle boundary distribution of the initial microstructure in addition to the stored dislocation density. This is discussed in more detail elsewhere.[13,24,26]

4.3. Transition Strain Characteristics

An interesting issue raised by this work is why the co-incidence of ε^* with ε_p seems to depend upon Z and composition (Figs. 8–10). In order to develop a rationale for this behaviour it is first necessary to consider why the softening behaviour becomes strain independent at higher strains. One obvious reason is that at higher strains the deformed microstructure attains a steady state. This necessarily leads to a steady state driving force for recrystallization. It is thus expected that the softening kinetics ought to become independent of strain once the steady state is reached. However, the present work, and many previous studies,[3,6,8,10,18,27] have shown that steady state softening commences at strains lower than this.

This "early" onset of strain independent softening behaviour can be rationalized if the following idealized view of DRX is assumed. This view has it that DRX grains nucleate at the boundaries of the pre-existing grains[28] and thus form a "necklace" structure surrounding a deformed core. Furthermore, it is assumed that once a small fraction of DRX has been attained, the average size of the DRX grains remains constant.[12,29] The DRX part of the structure there-

fore attains a "steady state" at strains considerably less than the strain to the steady state stress.

A steady state in the post deformation softening rate can therefore be expected to arise when the following two conditions are met: i) all of the nuclei for recrystallization are provided by the DRX part of the structure and ii) their distribution in space is similar to that for a full DRX structure. (Note that this assumes an unchanging growth rate.) These conditions can be attained in a 'partially' dynamically recrystallized structure if the core of deformed material in the grain interior is not too large. The critical size of the core, d^*_{def}, is expected to be a low multiple, c_1, of the steady state recrystallized grain size, d_{mdrx},[15,29] which in turn is known to be a multiple of the DRX grain size, d_{drx},[3,30] thus:

$$d^*_{def}=c_1 d_{mdrx}=c_2 d_{drx} \quad \text{.....(5)}$$

Now according to the present idealized view, the size of the deformed core, for spherical grains, can be given by:

$$d_{def}\approx d_0\sqrt[3]{1-X_{drx}} \quad \text{.....(6)}$$

To provide a link with the stress strain curve, we note that the strain to the flow stress peak is expected to scale with the kinetics of DRX. A rapid rate of DRX (*e.g.* at high temperatures) corresponds to a low strain to the peak stress. As a first approximation we can thus write:

$$X_{drx}=f_1(\varepsilon/\varepsilon_p) \quad \text{.....(7)}$$

A similar approach has been used previously to describe DRX kinetics[27,31–33] only in those cases the strain to 50% recrystallisation ($\varepsilon_{0.5}$) was employed in place of ε_p. Combining Eqs. (5) to (7) at the critical core size gives:

$$d_{drx}/d_0=f_2(\varepsilon^*/\varepsilon_p) \quad \text{.....(8)}$$

Thus it is expected that $\varepsilon^*/\varepsilon_p$ should vary with d_{drx}/d_0. Values for d_{drx} were obtained from published data[6,34,35] for grades similar to the three studied grades (and validated experimentally for a limited number of deformation conditions) and plotted against the experimentally obtained d_0, ε^* and ε_p in **Fig. 11**. It is apparent that, despite the disparity in their compositions, the data for the three grades seem to fall on a common curve. Additional data from the literature[3,8,10,11] is included in Fig. 11 and fall closely in line with the present results. This suggests that the differences in the relationship between ε^* and ε_p in the present work is geometric and arises as a consequence of differences in d_0 and d_{drx}.

It is interesting to note that values of $\varepsilon^*/\varepsilon_p$ significantly

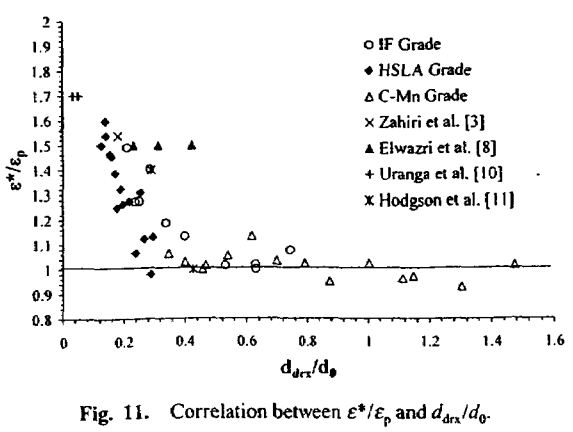

Fig. 11. Correlation between $\varepsilon^*/\varepsilon_p$ and d_{drx}/d_0.

below unity are not observed. This can be understood in terms of the stress. For strains below ε_p, an increase in strain is accompanied, by definition, by an increase in stress and therefore dislocation density. This, in turn, is expected to increase the rate of subsequent recrystallization. It is therefore not expected that ε^* would fall below ε_p.

5. Conclusions

The softening kinetics of three grades of steel (C–Mn, HSLA and IF) were analysed and compared, with particular focus on the transition from strain dependent to strain independent softening behaviour. It was found that at lower values of Z, the transition strain coincided closely with the peak strain. However, at higher Z values the transition strain began to deviate from the peak strain and, as Z increased, so too did this deviation. It was found that the relationship between peak strain and transition strain for a number of grades and deformation conditions could be quite accurately described using the ratio of the dynamically recrystallised grain size and the initial grain size. A hypothesis for the observed behaviour was proposed based on the volume fraction of dynamic recrystallisation required for strain independent softening.

Acknowledgements

This work was supported through Australian Research Council (ARC) funding. The authors thank BlueScope Steel for the supply of test materials and Ron Gloss and Carl Gruber for their technical support.

REFERENCES

1) T. Gladman: The Physical Metallurgy of Microalloyed Steels, The Institute of Materials, London, (1997), 235.
2) F. Siciliano, Jr.: Ph.D. Thesis, McGill University, Montreal, Canada, (1999).
3) S. H. Zahiri and P. D. Hodgson: *Mater. Sci. Technol.*, **20** (2004), 458.
4) P. Pauskar and R. Shivpuri: 40th MWSP, ISS, Warrendale, PA, (1998), 755.
5) C. Devadas, I. V. Samarasekera and E. B. Hawbolt: *Metall. Trans. A*, **22A** (1991), 335.
6) L. P. Karjalainen, T. M. Maccagno and J. J. Jonas: *ISIJ Int.*, **35** (1995), 1523.
7) J. J. Jonas: *ISIJ Int.*, **40** (2000), 731.
8) A. M. Elwazri, E. Essadiqi and S. Yue: *ISIJ Int.*, **44** (2004), 744.
9) D. Q. Bai, S. Yue and J. J. Jonas: Proc. of Thermomechanical Processing of Steel, Ottawa, ON, ed. by S. Yue and E. Essadiqi, MET SOC, Montreal, Canada, (2000), 669.
10) P. Uranga, A. I. Fernandez, B. Lopez and J. M. Rodriguez-Ibabe: *Mater. Sci. Eng. A*, A345 (2003), 319.
11) P. D. Hodgson, S. H. Zahiri and J. J. Whale: *ISIJ Int.*, **44** (2004), 1224.
12) P. D. Hodgson, D. C. Collins and B. Perret: 7th Int. Symp. on Physical Simulation, Dynamic Systems Inc. & NRIM Japan, Japan, (1997), 219.
13) C. Roucoules, P. D. Hodgson, S. Yue and J. J. Jonas: *Metall. Mater. Trans. A*, 25A (1994), 389.
14) G. F. Vander Voort: Metallography, Principles and Practise, ASM Int., Materials Park, OH, (1999).
15) C. M. Sellars: Hot Rolling and Forming Processes, ed. by C. M. Sellars and J. Davies, The Metals Society, London, (1980), 3.
16) A. I. Fernandez, P. Uranga, B. Lopez and J. M. Rodriguez-Ibabe: *Mater. Sci. Eng. A*, A361 (2003), 367.
17) N. D. Ryan and H. J. McQueen: *Can. Metall. Q.*, **29** (1990), 147.
18) S. H. Zahiri, S. M. Byon, S. Kim, Y. Lee and P. D. Hodgson: *ISIJ Int.*, 44 (2004), 1918.

19) J. J. Jonas: High Strength Low Alloy Steels, ed. by D. P. Dunne and T. Chandra, ASM, Materials Park, OH, (1984), 80.
20) S. F. Medina and J. E. Mancilla: *ISIJ Int.*, **36** (1996), 1063.
21) A. J. DeArdo: *Ironmaking Steelmaking*, **28** (2001), 138.
22) B. K. Panigrahi: *Bull. Mater. Sci.*, **24** (2001), 361.
23) C. M. Sellars: Thermomechanical Processing of Steel, Canada, ed. by S. Yue and E. Essadiqi, Met. Soc., Montreal, Canada, (2000), 3.
24) W. P. Sun and E. B. Hawbolt: *ISIJ Int.*, **37** (1997), 1000.
25) P. D. Hodgson and R. K. Gibbs: *ISIJ Int.*, **32** (1992), 1329.
26) S. Cho, K. Kang and J. J. Jonas: *ISIJ Int.*, **41** (2001), 63.
27) P. D. Hodgson: Ph.D. Thesis, University of Queensland, (1993)
28) F. J. Humphries and M. Hatherly: Recrystallization and Related Annealing Phenomena, Elsevier Science Ltd., Oxford, UK, (1995).
29) C. Roucoules, S. Yue and J. J. Jonas: Proc. of 1st Int. Conf. on Modelling of Metal Rolling Processes, Imperial College, London, UK, (1993), 165.
30) P. D. Hodgson, J. J. Jonas and S. Yue: Int. Conf. Grain Growth of Crystalline Materials, Trans. Tech. Publications Inc., Switzerland, (1991).
31) T. Senuma, H. Yada, Y. Matsumura and T. Futamura: *Tetsu-to-Hagané*, **79** (1984), 2112.
32) S. Nanba, M. Kitamura, M. Shimada, M. Katsumata, T. Inoue, H. Imamura, Y. Maeda and S. Hattori: *ISIJ Int.*, **32** (1992), 377.
33) A. Kirihata, F. Siciliano, Jr., T. M. Maccagno and J. J. Jonas: *ISIJ Int.*, **38** (1998), 187.
34) P. D. Hodgson: Thermec '97, ed. by T. Chandra and T. Sakai, TMS, Warrendale, PA, (1997), 121.
35) H. Yada: Proc. Int. Symp. Accelerated Cooling of Rolled Steel, Winnipeg, MB, Canada, ed. by G. E. Ruddle and A. F. Crawley, Pergamon Press, New York, (1987), 105.